Polymer 245 (2022) 124572

Contents lists available at ScienceDirect

Polymer

journal homepage: www.elsevier.com/locate/polymer

Study of two novel siloxane-containing polybenzoxazines with intrinsic low dielectric constant

Manlin Yuan [a], Xin Lu [a], Yudi Zhao [a], Shiao-Wei Kuo [b], Zhong Xin [a,*]

[a] State Key Laboratory of Chemical Engineering, School of Chemical Engineering, East China University of Science and Technology, Shanghai, 200237, People's Republic of China

[b] Department of Materials and Optoelectronic Science, National Sun Yat-Sen University, Kaohsiung, 804, Taiwan

ARTICLE INFO

Keywords:
Benzoxazine
Low dielectric
Siloxane
Intrinsic

ABSTRACT

The new generation of high-speed and low-loss electronic equipment requires the dielectric constant and dielectric loss of materials to be as low as possible. In this paper, two novel siloxane-containing benzoxazine monomers P-aptmds (1,3-bis(3-(6-(*tert*-butyl)-3,4-dihydro-2H-1,3-benzoxazine-3-yl)propyl)-1,1,3,3-tetramethyldisiloxane) and P-appdms (1,3-bis(3-(6-(*tert*-butyl)-3,4-dihydro-2H-1,3-benzoxazine-3-yl)propyl)-polydimethylsiloxane) with different lengths of dimethylsiloxane segments were successfully synthesized. It was noted that PP-appdms had excellent thermal stability due to the long dimethylsiloxane segments. Compared with PP-aptmds, the surface free energy and water absorption of PP-appdms was significantly lower. The static water contact angle of PP-appdms was 111.2° and the surface free energy was only 13.37 mN/m^2. Due to the presence of bulky *tert*-butyl groups and non-polar siloxane segments, both PP-aptmds and PP-appdms showed good dielectric properties with dielectric constant of 2.82 and 3.09 respectively.

1. Introduction

The widespread application of the fifth-generation mobile communication technology requires faster signal transmission and lower loss in electronic components [1,2]. Reducing the dielectric constant and dielectric loss of the resin matrix is quite important [3]. According to Debye's formula, the dielectric constant of a dielectric material is related to its polarizability and dipole density [4,5]. At present, the common measures used to reduce the dielectric constant of materials are as follows: (1) Introduce groups with low polarizability to reduce the overall polarizability of the material [6–8]; (2) Design molecular structures with large steric hindrance to reduce the overall dipole number density [9]; (3) Prepare porous materials to introduce air which is of extremely low dielectric constant [10,11].

According to the above strategies, a few kinds of polymers have been employed to prepare low dielectric constant (low-*k*) electronic materials. Wang et al. [12] modified the bisphenol A dicyanate ester with a novel fluorine-containing polyaryletherketone, and the $-CF_3$ groups with low polarizability improved the dielectric properties of the cyanate ester. Wang et al. [13] prepared a series of polyimide/aminoquinoline-functionalized graphene oxide nanocomposites, and the dielectric constant of polyimide was reduced from 3.37 to 2.96 at 1 MHz after adding the nanofiller which had a large free volume.

Polybenzoxazine resin has low intrinsic dielectric constant [14], low water absorption [15] and good thermal stability [16,17]. Moreover, benzoxazine monomers with special functional groups could be synthesized directly due to the excellent molecular design flexibility of polybenzoxazines, which could simplify the polymerization process [18]. Chen et al. [19] synthesized polybenzoxazines containing *tert*-butyl with nonpolar bulky rigid structure, which had good dielectric properties at 5 GHz and 10 GHz. Besides, bulky groups such as adamantane [20], carbazole [21] and polyhedral oligomeric silsesquioxane [22] were also introduced into the polybenzoxazine resin to optimize the dielectric properties by reducing the number density of dipoles. Due to the particularity of the Si–O–Si bond, organopolysiloxane has excellent thermal stability, flexibility and low surface tension [23,24]. The introduction of siloxane into the molecular structure of benzoxazine could improve its inherent brittleness and further enhance its hydrophobicity and thermal stability [25]. Zhang et al. copolymerized benzoxazine with polydimethylsiloxane and found that the cross-linked networks of the copolymer had large free volume which could decrease the dielectric constant and the degree of moisture absorption [26].

This work chose 4-*tert*-butylphenol with large sterically hindered

* Corresponding author.
E-mail address: xzh@ecust.edu.cn (Z. Xin).

https://doi.org/10.1016/j.polymer.2022.124572
Received 1 December 2021; Received in revised form 16 January 2022; Accepted 17 January 2022
Available online 1 February 2022

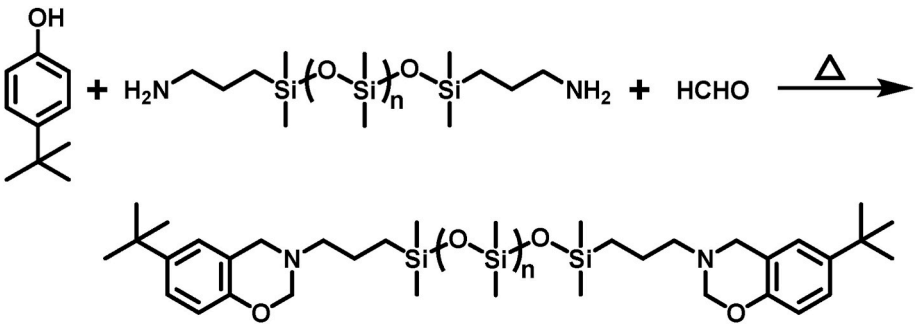

Scheme 1. Synthesis routes of P-aptmds (n = 0) and P-appdms (n ≈ 200).

tert-butyl group and aliphatic diamines containing dimethylsiloxane segments of different lengths as the raw materials to prepare two novel intrinsic low-*k* polybenzoxazine homopolymers. Their ring-opening polymerization process was characterized by *in-situ* FT-IR and differential scanning calorimetry. Afterwards, polybenzoxazine was prepared by step heat curing method. According to the standard IPC-TM-650-2.6.2.1, their water absorption performance was investigated [27]. A broadband dielectric impedance spectrometer was used to characterize their dielectric constant and dielectric loss.

2. Experimental section

2.1. Materials

Paraformaldehyde, 4-*tert*-butylphenol and sodium hydroxide were obtained from Shanghai Titan Scientific Co., Ltd. 1,3-bis(aminopropyl) tetramethyldisiloxane (APTMDS) and aminopropyl terminated polydimethylsiloxane (APPDMS, M_n = 15000) were purchased from Shanghai Macklin Biochemical Co., Ltd. Trichloromethane and hydrochloric acid (35.0–38.0 wt %) were purchased from Sinopharm Chemical Reagent Co., Ltd. All chemicals were of analytical grade and used as received.

2.2. Synthesis of benzoxazine monomers

Two benzoxazine monomers were both synthesized by one-step primary amine method. To synthesize P-aptmds (1,3-bis(3-(6-(*tert*-butyl)-3,4-dihydro-2H-1,3-benzoxazine-3-yl)propyl)-1,1,3,3-tetramethyldisiloxane), paraformaldehyde (0.16 mol, 4.800 g), APTMDS (0.04 mol, 9.940 g) and trichloromethane were added into a round-bottomed flask and heated to 60 °C. Subsequently, 4-*tert*-butylphenol (0.08 mol, 12.018 g) dissolved in trichloromethane was dropped into the flask. Then the mixture was heated to 80 °C and kept for 6 h. After cooling to room temperature, the resultant crude product was washed with NaOH aqueous, HCl aqueous and deionized water successively. Afterwards, the trichloromethane and water in the residual product were removed by vacuum distillation and lyophilizer to yield P-aptmds as a yellowish thick liquid.

The synthesis process of P-appdms (1,3-bis(3-(6-(*tert*-butyl)-3,4-dihydro-2H-1,3-benzoxazine-3-yl)propyl)-polydimethylsiloxane) was the same as that of P-aptmds except for replacing raw material APTMDS with APPDMS. The three raw materials were added according to the stoichiometric ratio. The synthesis route of benzoxazine monomers is illustrated in Scheme 1.

2.3. Preparation of polybenzoxazines

In order to prepare wafers with flat surface, the benzoxazine monomers were thermally cured stepwise by a mold casting method. P-aptmds and P-appdms were firstly poured into the mold, and then were placed into a vacuum drying oven at 70 °C for 1 h to remove bubbles which could be caused by air in the gap between mold and monomers. After that, they were placed in an oven and the curing process was as follows: 120 °C (1 h), 150 °C (1 h), 180 °C (1 h), 200 °C (1 h), 210 °C (1 h) and 220 °C (6 h). Finally, samples were placed in a desiccator and cooled to room temperature naturally to obtain polybenzoxazines PP-aptmds and PP-appdms [28].

2.4. Characterizations

Nuclear magnetic resistance spectroscopy (NMR). ^{1}H NMR, ^{13}C NMR and ^{29}Si NMR spectra were recorded on a Bruker NMR spectrometer (ASCEND, 600 MHz , America). All samples were dissolved in deuterated chloroform.

Fourier transform infrared spectroscopy (FT-IR). Spectroscopy was measured with a Thermo Fisher Scientific Nicolet IS10 FT-IR analyzer (America), and all samples were tested by the method of potassium bromide tablet. Spectra in the range of 4000–400 cm^{-1} were scanned 32 times with a resolution of 4 cm^{-1}. The temperature was increased from 30 °C to 300 °C for *in-situ* FT-IR testing, and the heating rate was 10 °C/min.

Differential scanning calorimetry (DSC). The thermal behavior of benzoxazines and polybenzoxazines were characterized by a TA differential scanning calorimetry (Q2000, America). The 3–5 mg samples were measured in an aluminum crucible and heated to 300 °C at a rate of 10 °C/min under nitrogen atmosphere.

Thermogravimetric analysis (TGA). The thermal properties were performed using a TA thermogravimetric analyzer (SDT Q600, America). The samples were examined from 40 °C to 800 °C at a rate of 10 °C/min under nitrogen atmosphere.

Scanning electron microscopy (SEM). Images were collected using a FEI scanning electron microscopy (Nova NanoSEM 450, America) operated at 5 KV. The samples were sprayed with platinum for 80 s in the vacuum coater.

Surface properties measurement. The static contact angle and surface free energy of polybenzoxazines were tested with a contact angle measuring instrument (Dataphysics OCA20, Germany). The liquid used in the test includes water, diiodomethane and ethylene glycol, and the amount of each drop was 6 μL. The calculation of surface free energy adopted the OWRK model.

Mechanical properties measurement. The mechanical properties of PP-aptmds and PP-appdms were tested on the basis of ASTM test methods, with a universal testing machine (MTS Systems CMT4204, China).

Water absorption measurement. The water absorption test of PP-aptmds was implemented according to the standard IPC-TM-650-2.6.2.1. Samples (length: 5.08 mm, width: 5.08 mm, thickness: 1 mm) were conditioned by drying in an oven for 1 h at 110 °C, cooled to room temperature in a desiccator, weighted and recorded as W_1. The conditioned samples were completely immersed in deionized water maintained at 23 ± 1.1 °C for 24 h. After that, the weight of samples was recorded as W_2. The percentage of water absorption was calculated

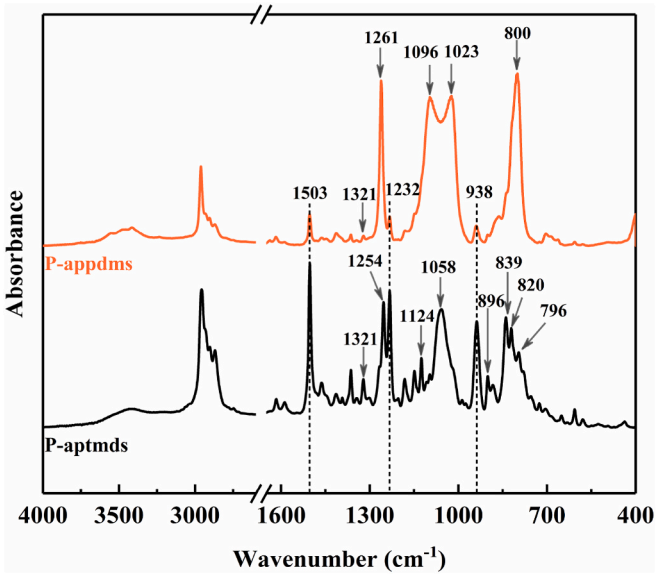

Fig. 1. FT-IR spectra of benzoxazine monomers.

using the following equation:

$$\text{The percentage of water absorption} = \frac{W_2 - W_1}{W_1} \times 100\%$$

Dielectric properties measurement. The dielectric properties of PP-aptmds and PP-appdms were tested using a Novocontrol broadband dielectric spectrometer (concept 40, Germany) at frequency from 100 Hz to 1 MHz. The samples were dried before measurements and then tested at 25 °C.

3. Results and discussion

3.1. Structural characterizations of benzoxazine monomers

The structures of benzoxazine monomers were characterized by FT-IR. Absorption peaks at 938 cm^{-1},1124 cm^{-1}, 1232 cm^{-1} and 1321 cm^{-1} are detected in the spectra of Fig. 1, corresponding to the C–H out-of-plan bending vibration of the oxazine ring, the stretching vibration of C–N–C, the anti-symmetric stretching vibration of Ar-O-C and the swing vibration of methylene in the oxazine ring respectively. The positions of the absorption peaks related to the oxazine ring in the two monomers are basically the same. However, due to the high content of siloxane in P-appdms, the intensity of the absorption peaks associated with the oxazine ring are relatively small. The C–H out-of-plan bending vibration peaks of the 1,2,4-trisubstituted benzene ring appear at 820 cm^{-1} and 896 cm^{-1}. The absorption peaks at 1023 cm^{-1} and 1096 cm^{-1} in P-appdms and 1058 cm^{-1} in P-aptmds are all stretching vibration peaks of Si–O–Si. The absorption peaks at 1261 cm^{-1} in P-appdms and 1254 cm^{-1} in P-aptmds are both bending vibration peaks of Si–CH_3. The absorption peaks at 800 cm^{-1} in P-appdms and 839 cm^{-1} and 796 cm^{-1} in P-aptmds are all stretching vibration peaks of Si–C.

After that, ^{1}H NMR, ^{13}C NMR and ^{29}Si NMR were employed to characterize the structure of benzoxazine monomers further, and the results are shown in Fig. 2. In Fig. 2(a), the multiplet between 6.6 ppm and 7.1 ppm (a) are the response peaks of the proton in the benzene ring; resonances at 4.8 ppm (b) and 3.9 ppm (c) are observed which are associated with the proton in the oxazine ring; resonances at 2.7 ppm (d), 1.5 ppm (e) and 0.5 ppm (f) correspond to the proton in the methylene group on the aliphatic chain; resonance peaks at 1.2 ppm (g) and 0 ppm (h) represent the proton in the *tert*-butyl group in the silicon atom and the methyl group, respectively. The positions of response peaks of P-appdms in Fig. 2(b) are basically the same to P-aptmds. The signals at 82.0 ppm, 54.3 ppm and 81.3 ppm, 53.6 ppm in the ^{13}C NMR spectra of Fig. 2 (c, d) also prove the existence of the oxazine ring. In Fig. 2 (e), the ^{29}Si NMR spectrum of P-aptmds only have one response peak, which proves that the silicon atoms in benzoxazine only have one chemical environment. The silicon atom in P-appdms should have two chemical environments, including the chain end and the chain backbone. However, since the number of silicon atoms in the chain backbone is far more than those at the chain end, only one response peak could be seen in Fig. 2(f).

3.2. Curing behavior of benzoxazine monomers

The curing behavior of the benzoxazine monomers was studied by DSC, and the test results are shown in Fig. 3. The DSC curve of P-aptmds shows a sharp exothermic peak in the range of 224.45 °C–278.34 °C, which corresponds to the ring-opening polymerization process. The exothermic peak onset temperature T_{on} is 224.45 °C, and the peak temperature T_{peak} is 259.19 °C. Compared with P-aptmds, P-appdms has a lower T_{on} and a broader exothermic peak, and its T_{peak} is 239.58 °C. After curing, the DSC curves of PP-aptmds and PP-appdms no longer show exothermic peaks, indicating that they are all completely cured.

The *in-situ* FT-IR was utilized to characterize the structural changes during the curing of benzoxazine monomers, and the results are shown in Fig. 4. For quantitative analysis, all curves were normalized based on the symmetric deformation of C–H in methyl group at 1364 cm^{-1}. In Fig. 4(a), as the temperature gradually increases, the response peaks at 938 cm^{-1}, 1232 cm^{-1} and 1321 cm^{-1} related to the oxazine ring gradually weaken. When the temperature rises to 280 °C, these characteristic peaks of P-aptmds disappear completely, indicating that the oxazine ring has completely opened at this time, which is consistent with the results of the DSC curve. In Fig. 4(b), the response peaks related to the oxazine ring in P-appdms also decrease with increasing temperature and disappear when the temperature is 230 °C.

3.3. Thermal properties of polybenzoxazines

Fig. 5 shows the weight loss of polybenzoxazines during heating under nitrogen atmosphere, and the data are recorded in Table 1. The temperature when the weight loss is 1%, 5%, and 10% are recorded as $T_{1\%}$, $T_{5\%}$, $T_{10\%}$ respectively, and the residual carbon rate at 800 °C is recorded as CY. It can be seen from Fig. 5(a) that as the temperature increases, the weight loss of PP-aptmds is significantly more than that of PP-appdms. The $T_{1\%}$, $T_{5\%}$, and $T_{10\%}$ of PP-aptmds are 248.20 °C, 288.78 °C, and 311.37 °C, while those of PP-appdms are 342.71 °C, 430.53 °C, and 474.66 °C. Since the Si–O bond has a high bond energy (460 kJ/mol), the extension of the siloxane chain could markedly improve the thermal stability of polybenzoxazine.

The derivative of weight loss of PP-aptmds in Fig. 5(b) indicates that there are at least four weight loss events. The weight loss when the temperature is lower than 400 °C generally corresponds to the evaporation of the amine compound and the Schiff base formed by the cleavage of the C–N [29]. Because the cleavage products with long siloxane chains are more difficult to volatilize, the first two weight loss events which occur at approximately 300 °C and 370 °C almost disappear in the DTG curve of PP-appdms.

3.4. Morphology and surface properties of polybenzoxazines

The macroscopic and microscopic features of the cured polymers are shown in Fig. 6. PP-aptmds obtained from APTMDS was rufous in color (a), while PP-appdms synthesized by APPDMS was darker in color (c). The color of the polymer tends to deepen as the length of the siloxane segment increases. The long siloxane segment in PP-appdms can remarkably improve its flexibility. The PP-appdms was prepared into a rectangular parallelepiped piece with a size of 20 mm × 10 mm × 2 mm and could be folded easily without breaking (e), while PP-aptmds

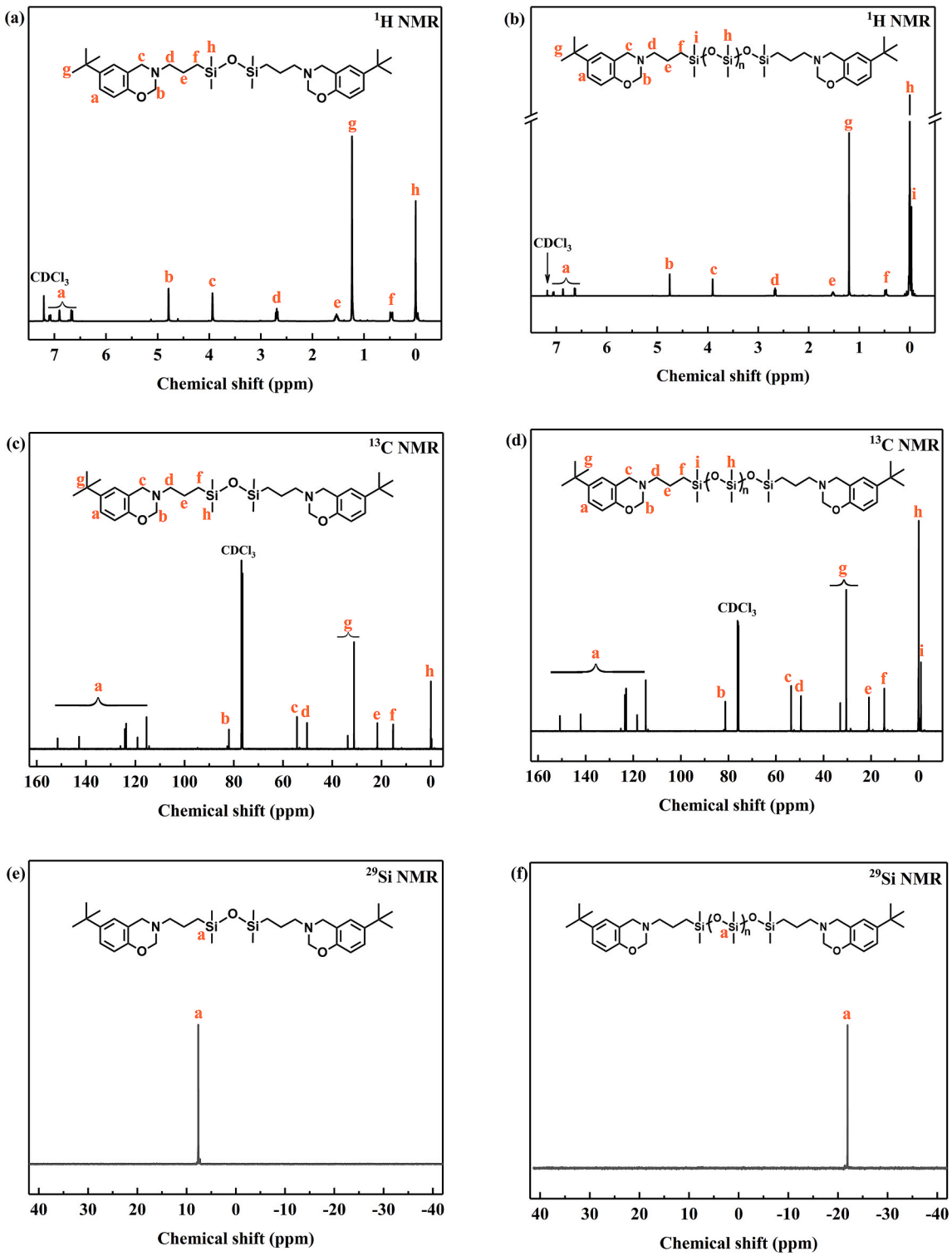

Fig. 2. (a, b) ^{1}H NMR spectra, (c, d) ^{13}C NMR spectra and (e, f) ^{29}Si NMR spectra of benzoxazine monomers.

possessed strong rigidity and could not be folded. The surface of polybenzoxazines were observed by SEM. The surface of PP-aptmds (b) and PP-appdms (d) are both smooth and flat, which proves that the two benzoxazine monomers both have superior film forming property.

Polybenzoxazine is a resin with low surface free energy because of the dense hydrogen bond (HB) network. The static contact angles of polybenzoxazines to water, diiodomethane and ethylene glycol were tested respectively. The surface free energy was calculated by OWRK model equation (equation (1)) [30].

$$\frac{0.5(1+cos\theta)\gamma_L}{\sqrt{\gamma_L^d}} = \sqrt{\gamma_S^d} + \sqrt{\gamma_S^p}\frac{\sqrt{\gamma_L^p}}{\sqrt{\gamma_L^d}} \quad (1)$$

Where θ is the static contact angle (°); γ is the surface tension (mN/m^2); superscripts d and p represent the dispersive part and the polar part of γ, respectively; subscripts S and L respectively denote the liquid and solid tested. As shown in Table 2, the static water contact angles of PP-aptmds and PP-appdms are 99.9° and 111.2° respectively, both of which are

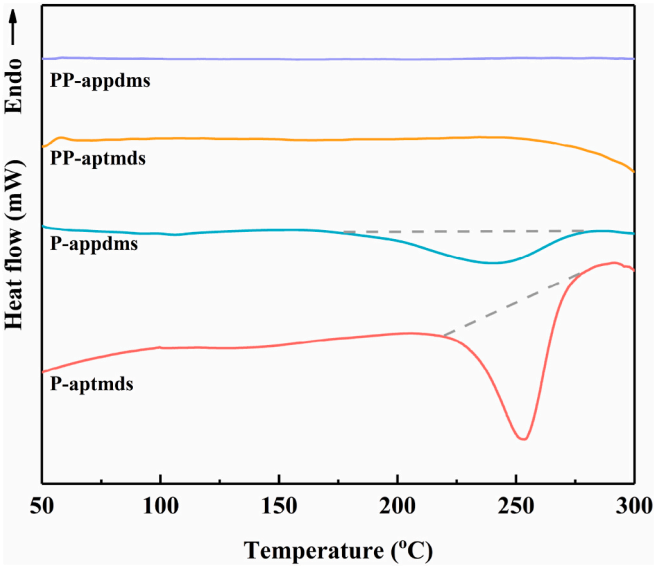

Fig. 3. DSC curves of P-aptmds, P-appdms, PP-aptmds and PP-appdms.

hydrophobic. It was calculated that the surface free energy of PP-aptmds and PP-appdms are 18.87 mN/m^2 and 13.37 mN/m^2 respectively. Such difference could be attributed to the difference in the length of the siloxane segment which is known for hydrophobicity.

Since the dielectric constant of water at room temperature is 80 [31], reducing the water absorption rate of the material could reduce the dielectric constant and increase the dielectric stability availably. According to the standard IPC-TM-650-2.6.2.1, the water absorption rate of PP-aptmds and PP-appdms was tested. The water absorption rate of PP-aptmds is as low as 0.282%, while the water absorption rate of PP-appdms is only 0.025%. Obviously, the presence of long siloxane segments significantly decreases the water absorption rate of the polybenzoxazine.

3.5. *Mechanical properties of polybenzoxazines*

The tensile strength and break elongation of PP-aptmds and PP-

Table 1
Thermal properties data of polybenzoxazines.

Samples	$T_{1\%}$ (°C)	$T_{5\%}$ (°C)	$T_{10\%}$ (°C)	CY (%)
PP-aptmds	248.20	288.78	311.37	10.38
PP-appdms	342.71	430.54	474.66	14.70

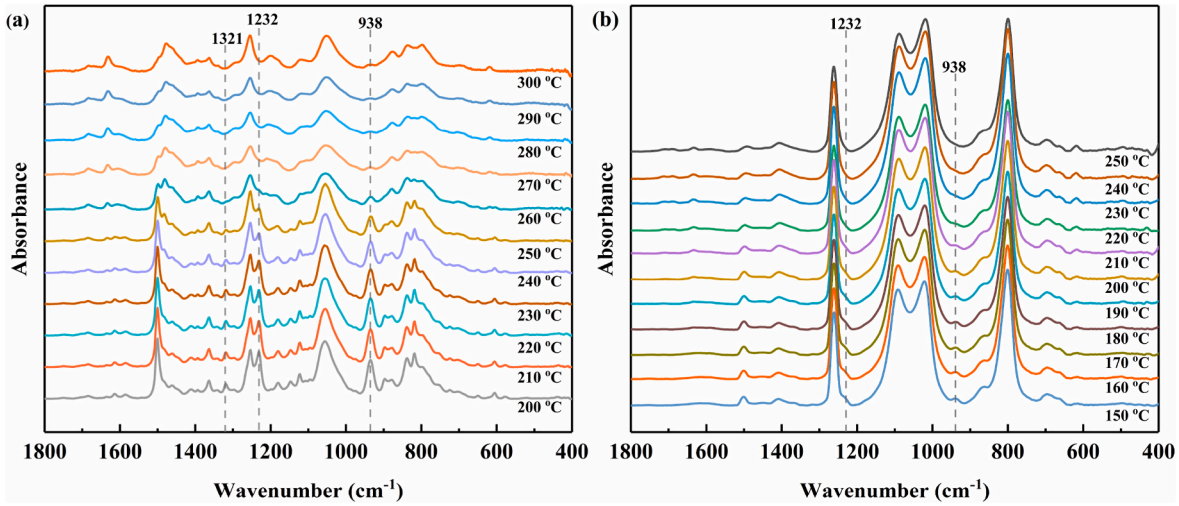

Fig. 4. *In-situ* FT-IR spectra during the curing process of (a) P-aptmds and (b) P-appdms.

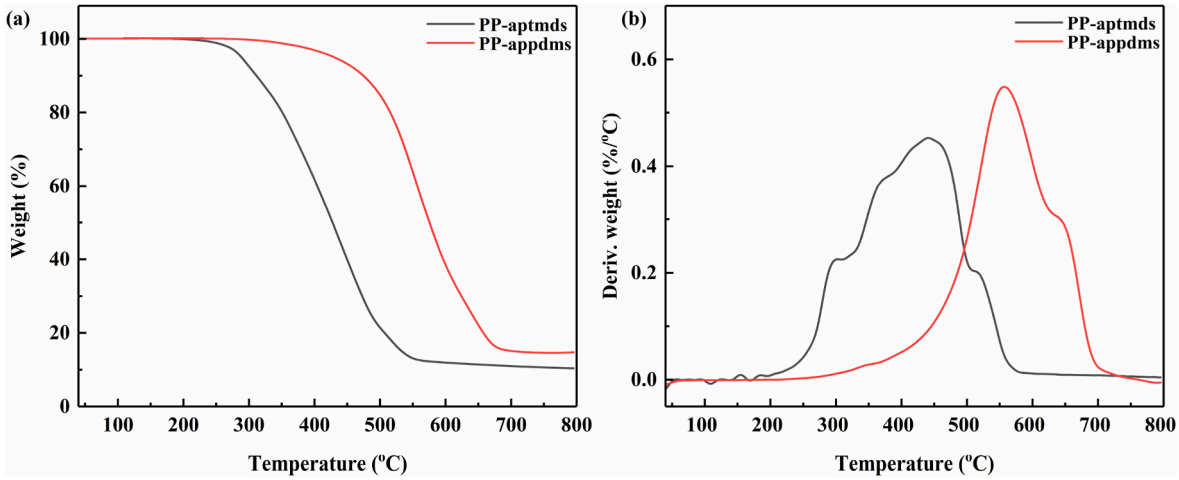

Fig. 5. (a) TGA curves and (b) DTG curves of PP-aptmds and PP-appdms.

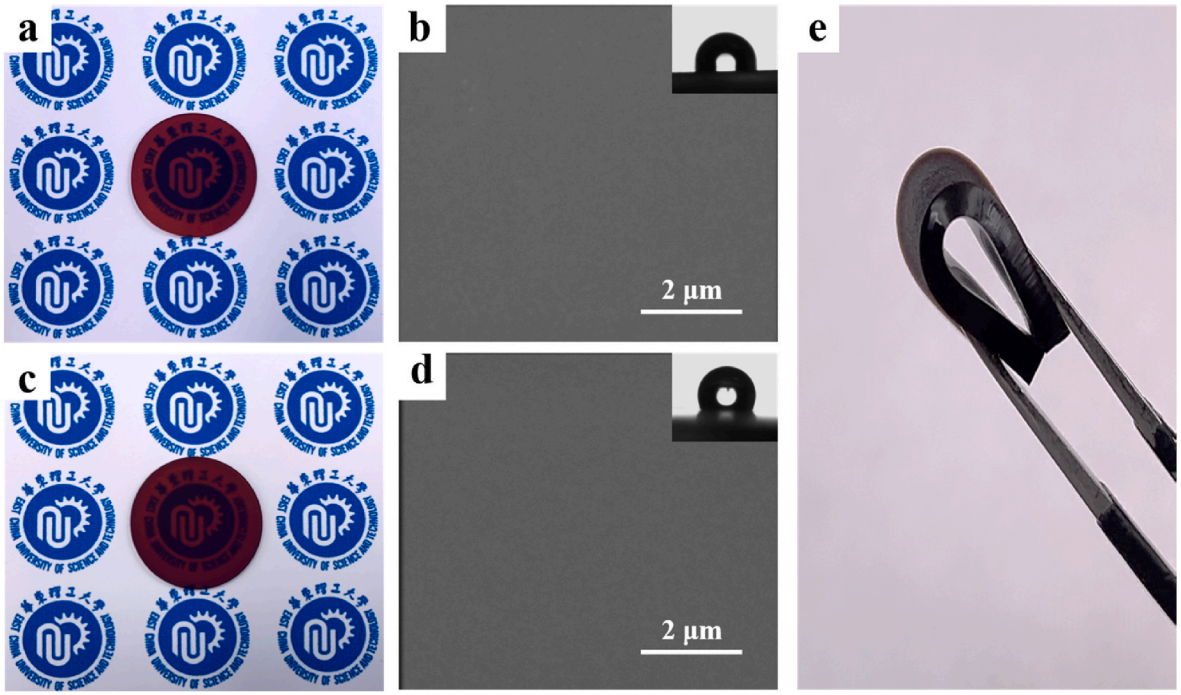

Fig. 6. Morphology of (a, b) PP-aptmds and (c, d, e) PP-appdms (the inset is the corresponding static water contact angle diagram).

Table 2
Surface properties of polybenzoxazines.

samples	static contact angle (°)			surface energy (mN/m^2)	water absorption (%)
	Water	diiodomethane	ethylene glycol		
PP-aptmds	99.9	89.5	65.9	18.87	0.282
PP-appdms	111.2	95.7	86.6	13.37	0.025

Table 3
Mechanical properties of PP-aptmds and PP-appdms.

Samples	tensile strength (MPa)	break elongation (%)
PP-aptmds	11.80	2.61
PP-appdms	0.03	68.15

appdms are shown in Table 3. PP-aptmds has a tensile strength of 11.80 MPa and a break elongation of 2.61%. Compared with PP-aptmds, PP-appdms has a higher proportion of flexible chains, namely siloxane chains, in the cross-link network. Therefore, the toughness of PP-appdms is significantly improved, and the break elongation is 68.15%. In addition, the long siloxane segments can also lead to a decrease in the crosslinking density of polybenzoxazines, for which reason PP-appdms has a low tensile strength with 0.03 MPa.

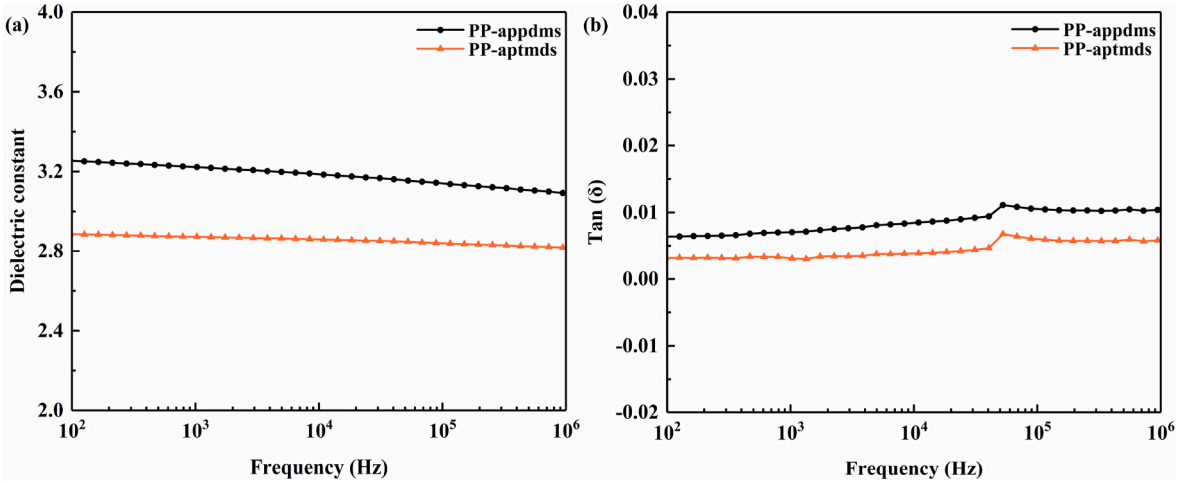

Fig. 7. (a) Dielectric constant and (b) dielectric loss curves of polybenzoxazines.

Table 4
Dielectric properties of polybenzoxazines.

Samples	dielectric constant (1 MHz)	tan (δ) (1 MHz)	ref.
PC-s	2.99	0.0096	[15]
Poly(*o*TFA-ddm)	2.84	0.019	[32]
BZPOSS	2.80	0.0400	[33]
BPAF-ph	3.54	0.0080	[34]
Poly(*o*HPNI-oda)	2.58	0.002	[26]
Poly(*o*HPNI-oda-PDMS)	2.29	0.002	[26]
PP-appdms	3.02	0.01038	this work
PP-aptmds	2.82	0.00581	this work

3.6. Dielectric properties of polybenzoxazines

A broadband dielectric impedance spectrometer was used to characterize the dielectric constant and dielectric loss of polybenzoxazine between 100 Hz and 1 MHz. The results are shown in Fig. 7. As the frequency increases, the dielectric constant of PP-appdms gradually decreases from 3.25 to 3.09, while the dielectric constant of PP-aptmds decreases from 2.89 to 2.82. In addition, the dielectric loss of PP-aptmds and PP-appdms at 1 MHz are 0.00581 and 0.01038 respectively. Therefore, the huge *tert*-butyl group, non-polar siloxane segment and the special HB network of polybenzoxazines endow PP-aptmds and PP-appdms with good dielectric properties. In addition, PP-aptmds and PP-appdms are compared with intrinsic low-*k* polybenzoxazines reported in the literature. As shown in Table 4, PP-aptmds has a relatively low dielectric constant and tan (δ), which has a relatively large application potential in the field of low-*k* electronic materials.

It is worth noting that the dielectric constant and dielectric loss of PP-appdms have slightly decreased. The increase in the length of the siloxane segments could decrease the crosslink density and weaken the HB network of polybenzoxazines, which causes the deterioration of the dielectric loss [35]. The decrease in crosslink density could also increase the orientation polarization of molecular segments, which would increase the dielectric constant of PP-appdms [36].

Most of the hydroxyl groups in polybenzoxazines could participate in the formation of the HB network which are difficult to be polarized. In order to characterize the influence of long siloxane segments on the HB network, the Gaussian equation was used to fit the FT-IR curves of polybenzoxazines in the range of 2000 cm^{-1} to 4000 cm^{-1}, and the results are shown in Fig. 8. There are three kinds of HB in the structure of PP-aptmds and PP-appdms, including OH···N and $O^{-}\cdots H^{+}N$ intra- HB and OH···O inter- HB. Fig. 9 shows the cross-linked network and HB structure of polybenzoxazines. As shown in Fig. 9, OH···N HB and $O^{-}\cdots H^{+}N$ HB both have a relatively stable six-member ring structure which is difficult to be polarized. The electronic cloud of OH···O HB is more delocalized and more likely to be polarizable [37]. The long siloxane segments not only weaken the overall hydrogen bond network, but also reduce the proportion of intra- HB. Therefore, both PP-aptmds and PP-appdms show good dielectric properties, while the dielectric properties of PP-appdms decrease slightly.

4. Conclusions

In summary, two novel intrinsic low-*k* polybenzoxazines PP-aptmds and PP-appdms with *tert*-butyl and dimethylsiloxane were successfully prepared. The FT-IR and NMR results of two monomers demonstrated the existence of the oxazine ring and the overall molecular structure. The existence of long siloxane chains improves the thermal stability and hydrophobicity of polybenzoxazine. Compared with PP-aptmds, the $T_{1\%}$ of PP-appdms has increased from 248.20 °C to 342.71 °C, and the water absorption has been reduced from 0.282% to 0.025%. Both PP-aptmds and PP-appdms are hydrophobic, and their surface free energy are 18.87 mN/m^2 and 13.37 mN/m^2 respectively. The incorporation of dimethylsiloxane segment and *tert*-butyl leads to polybenzoxazines have good dielectric properties. The dielectric constant of PP-aptmds is 2.82

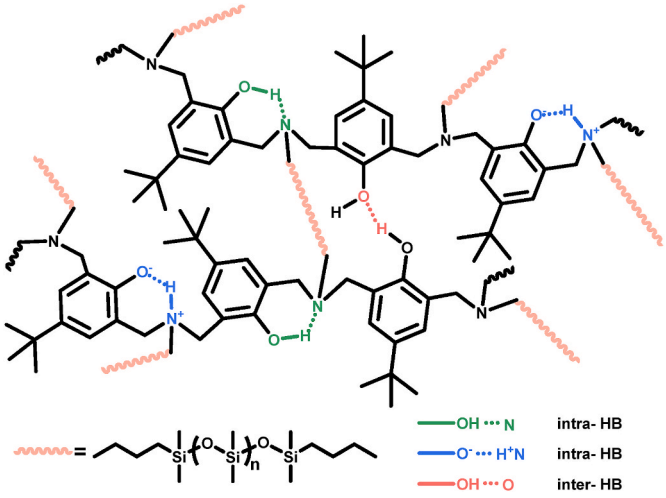

Fig. 9. Network structures for HB in polybenzoxazines.

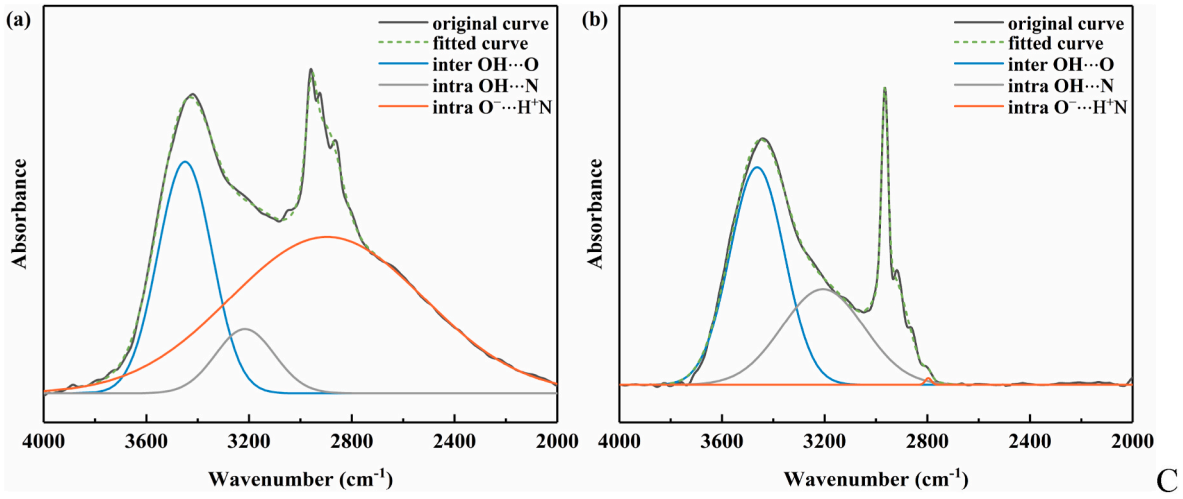

Fig. 8. Curve fitting for the FT-IR spectra of (a) PP-aptmds and (b) PP-appdms.

at 1 MHz. However, the extension of the siloxane chains decreases the crosslink density and weakens the HB network, causing a deterioration in the dielectric properties of PP-appdms.

CRediT authorship contribution statement

Manlin Yuan: Methodology, Investigation, Data curation, Visualization, Formal analysis, Writing – original draft, Writing – review & editing. **Xin Lu:** Conceptualization, Data curation, Project administration, Writing – review & editing. **Yudi Zhao:** Validation, Writing – review & editing, Resources. **Shiao-Wei Kuo:** Writing – review & editing. **Zhong Xin:** Funding acquisition, Supervision.

Declaration of competing interest

The authors declare that they have no known competing financial interests or personal relationships that could have appeared to influence the work reported in this paper.

Acknowledgements

This work was supported by Innovation Program of Shanghai Municipal Education Commission (2019-01-07-00-02-E00061), the Shanghai Municipal Science and Technology Commission (21520761100), National Nature Science Foundation of China (21776091), the Fundamental Research Funds for the Central Universities (JKA012116021) and the Open Project of State Key Laboratory of Chemical Engineering (SKL-ChE-21C07).

References

[1] J. Guo, H. Wang, C. Zhang, Q. Zhang, H. Yang, MPPE/SEBS composites with low dielectric loss for high-frequency copper clad laminates applications, Polymers (Basel) 12 (9) (2020) 1875–1886.
[2] Y.-M. Choi, J. Jung, A.S. Lee, S.S. Hwang, Photosensitive hybrid polysilsesquioxanes for etching-free processing of flexible copper clad laminate, Compos. Sci. Technol. 201 (2021), 108556.
[3] L. Tang, J. Zhang, Y. Tang, Y. Zhou, Y. Lin, Z. Liu, J. Kong, T. Liu, J. Gu, Fluorine/adamantane modified cyanate resins with wonderful interfacial bonding strength with PBO fibers, Compos. B Eng. 186 (2020), 107827.
[4] P.A. Kohl, Low-dielectric constant insulators for future integrated circuits and packages, Annu Rev Chem Biomol Eng 2 (2011) 379–401.
[5] F. Fu, D. Wang, M. Shen, S. Shang, Z. Song, J. Song, Preparation of planar and hydrophobic benzocyclobutene-based dielectric material from biorenewable rosin, J. Appl. Polym. Sci. 137 (26) (2020) 48831–48839.
[6] H. Min, B. Kang, Y.S. Shin, B. Kim, S.W. Lee, J.H. Cho, Transparent and colorless polyimides containing multiple trifluoromethyl groups as gate insulators for flexible organic transistors with superior electrical stability, ACS Appl. Mater. Interfaces 12 (16) (2020) 18739–18747.
[7] P. Pattharasiriwong, C. Jubsilp, P. Mora, S. Rimdusit, Dielectric and thermal behaviors of fluorine-containing dianhydride-modified polybenzoxazine: a molecular design flexibility, J. Appl. Polym. Sci. 134 (33) (2017) 45204–45211.
[8] R. Yang, B. Hao, L. Sun, K. Zhang, Cross-linked poly(benzoxazole-co-siloxane) networks with high thermal stability and low dielectric constant based on a new ortho-amide functional benzoxazine, J. Appl. Polym. Sci. 138 (6) (2020) 49792–49799.
[9] Z. Wang, M. Zhang, E. Han, H. Niu, D. Wu, Structure-property relationship of low dielectric constant polyimide fibers containing fluorine groups, Polymer 206 (2020), 122884.
[10] J.L. Cashman, B.N. Nguyen, B. Dosa, M.A.B. Meador, Flexible polyimide aerogels derived from the use of a neopentyl spacer in the backbone, ACS Appl. Polym. Mater. 2 (6) (2020) 2179–2189.
[11] P. Zhang, K. Zhang, X. Chen, S. Dou, J. Zhao, Y. Li, Mechanical, dielectric and thermal properties of polyimide films with sandwich structure, Compos. Struct. 261 (2021), 113305.
[12] C. Wang, Y. Tang, Y. Zhou, Y. Zhang, J. Kong, J. Gu, J. Zhang, Cyanate ester resins toughened with epoxy-terminated and fluorine-containing polyaryletherketone, Polym. Chem. 12 (26) (2021) 3753–3761.
[13] T. Wang, J. Li, F. Niu, A. Zhong, J. Liu, W. Liu, L. Shan, G. Zhang, R. Sun, C.-P. Wong, Low-temperature curable and low-dielectric polyimide nanocomposites using aminoquinoline-functionalized graphene oxide Nanosheets, Compos. B Eng. 228 (2022), 109412.
[14] W. Cai, Z. Wang, Z. Shu, W. Liu, J. Wang, J. Qiu, Development of a fully bio-based hyperbranched benzoxazine, Polym. Chem. 12 (47) (2021) 6894–6902.
[15] Y. Zhao, M. Yuan, L. Wang, X. Lu, Z. Xin, Preparation of bio-based polybenzoxazine/pyrogallol/polyhedral oligomeric silsesquioxane nanocomposites: low dielectric constant and low curing temperature, Macromol. Mater. Eng. (2021), 2100747.
[16] X. Zhang, M.G. Mohamed, Z. Xin, S.-W. Kuo, A tetraphenylethylene-functionalized benzoxazine and copper(II) acetylacetonate form a high-performance polybenzoxazine, Polymer 201 (2020), 122552.
[17] M.G. Mohamed, T.-C. Chen, S.-W. Kuo, Solid-state chemical transformations to enhance gas capture in benzoxazine-linked conjugated microporous polymers, Macromolecules 54 (12) (2021) 5866–5877.
[18] M.G. Mohamed, S.-W. Kuo, Crown ether-functionalized polybenzoxazine for metal ion adsorption, Macromolecules 53 (7) (2020) 2420–2429.
[19] J. Chen, M. Zeng, Z. Feng, T. Pang, Y. Huang, Q. Xu, Design and preparation of benzoxazine resin with high-frequency low dielectric constants and ultralow dielectric losses, ACS Appl. Polym. Mater. 1 (4) (2019) 625–630.
[20] S. Wang, J. Mao, L. Zhang, Y. Zheng, Y. Cheng, Development of adamantane-containing polybenzoxazines for dielectric interlayers applications, IEEE Trans. Dielectr. Electr. Insul. 27 (3) (2020) 714–721.
[21] V. Selvaraj, K.P. Jayanthi, M. Alagar, Development of biocomposites from agro wastes for low dielectric applications, J. Polym. Environ. 26 (9) (2018) 3655–3669.
[22] X. Li, J. Feng, S. Zhang, Y. Tang, X. Hu, X. Liu, X. Liu, Epoxy/benzoxazinyl POSS nanocomposite resin with low dielectric constant and excellent thermal stability, J. Appl. Polym. Sci. 138 (8) (2020) 49887–49895.
[23] M. Guo, Y. Huang, J. Cao, G. Sun, X. Zhao, J. Zhang, S. Feng, Recyclable sulfone-containing polymers via ring-opening polymerization of macroheterocyclic siloxane monomers: synthesis, properties and recyclability, Polym. Chem. 10 (45) (2019) 6166–6173.
[24] H. Lu, Z. Hu, D. Wang, K. Chen, S. Feng, Self-recoverable dual-network silicon elastomer applied in cell adhesives, Acs Appl. Polym. Mater. 1 (11) (2019) 2826–2832.
[25] M.G. Mohamed, S.W. Kuo, Functional silica and carbon nanocomposites based on polybenzoxazines, Macromol. Chem. Phys. 220 (1) (2019), 1800306.
[26] K. Zhang, X. Yu, S.-W. Kuo, Outstanding dielectric and thermal properties of main chain-type poly(benzoxazine-co-imide-co-siloxane)-based cross-linked networks, Polym. Chem. 10 (19) (2019) 2387–2396.
[27] J. Li, H. Zhang, D. Ying, Y. Wang, T. Sun, J. Jia, In plasma catalytic oxidation of toluene using monolith CuO foam as a catalyst in a wedged high voltage electrode dielectric barrier discharge reactor: influence of reaction parameters and byproduct control, Int. J. Environ. Res. Publ. Health 16 (5) (2019) 711–724.
[28] Z. Xin, M. Yuan, X. Lu, Preparation method and application of silicon-containing low-dielectric polybenzoxazine resin. Application Number: 202111245188.2, China.
[29] Y.L. Hong, I. Hatsuo, Structural effects of phenols on the thermal and thermo-oxidative degradation of polybenzoxazines, Polymer 40 (1999) 4365–4376.
[30] H. Yao, X. Lu, Z. Xin, X. Li, C. Chen, Y. Cao, Two novel eugenol-based difunctional benzoxazines: synthesis and properties, Colloids Surf. A Physicochem. Eng. Asp. 616 (2021), 126209.
[31] Y. Ma, Z. He, Z. Liao, J. Xie, H. Yue, X. Gao, Facile strategy for low dielectric constant polyimide/silsesquioxane composite films: structural design inspired from nature, J. Mater. Sci. 56 (12) (2021) 7397–7408.
[32] K. Zhang, L. Han, P. Froimowicz, H. Ishida, A smart latent catalyst containingo-trifluoroacetamide functional benzoxazine: precursor for low temperature formation of very high performance polybenzoxazole with low dielectric constant and high thermal stability, Macromolecules 50 (17) (2017) 6552–6560.
[33] S. Zhang, Y. Yan, X. Li, H. Fan, Q. Ran, Q. Fu, Y. Gu, A novel ultra low-k nanocomposites of benzoxazinyl modified polyhedral oligomeric silsesquioxane and cyanate ester, Eur. Polym. J. 103 (2018) 124–132.
[34] D. Ren, M. Xu, S. Chen, X. Xu, S. Zhang, M. Han, X. Liu, Curing reaction and properties of a kind of fluorinated phthalonitrile containing benzoxazine, Eur. Polym. J. 159 (2021), 110715.
[35] M. Zeng, J. Chen, Q. Xu, Y. Huang, Z. Feng, Y. Gu, A facile method for the preparation of aliphatic main-chain benzoxazine copolymers with high-frequency low dielectric constants, Polym. Chem. 9 (21) (2018) 2913–2925.
[36] Y. Mo, L. Yang, W. Hou, T. Zou, Y. Huang, R. Liao, Preparation of cellulose insulating paper with low dielectric constant by BTCA esterification crosslinking, Macromol. Mater. Eng. 305 (6) (2020).
[37] S. Zhang, Q. Ran, Q. Fu, Y. Gu, Thermal responsiveness of hydrogen bonding and dielectric property of polybenzoxazines with different Mannich bridge structures, Polymer 175 (2019) 302–309.